Methodology for Residual Stress Analysis in Aluminum Alloy 2024 Plates after Double-Sided Spherical Indentation ('Dimpling')

Igor A. Zorin[1, a)], Eugene S. Statnik[1,2,3], Eugene N. Prokopev[2], Alexey I. Salimon[1,2,3], Vladimir S. Pisarev[4], Svyatoslav I. Eleonsky[4], Andrey I. Shtypel[2] and Alexander M. Korsunsky[1,3]

[1]*Skolkovo Institute of Science and Technology (Skoltech), Moscow, Russia*
[2]*National University of Science and Technology 'MISIS' (NUST MISIS), Moscow, Russia*
[3]*CASM&T, Moscow Aviation Institute (MAI), Moscow, Russia*
[4]*The Zhukovsky Central Aero-Hydrodynamics Institute (TsAGI), Moscow, Russia*

[a)] Corresponding author: igor.zorin@skoltech.ru

Abstract. Double-sided spherical indentation ('dimpling') is an effective method of creating localized compressive residual stress in ductile metals to improve fatigue strength. Despite the proven effectiveness of this treatment, some aspects of the process remain insufficiently understood. The purpose of the present study is to develop an accessible means of analyzing deformations and stresses after the double dimpling treatment using the Digital Image Correlation (DIC) technique. Samples of 2024-T6 aluminum alloy were treated using a hydraulic rig, and the deformation increment was determined by DIC using a bespoke enclosure by a smartphone camera with LED lighting. A three-point kinematic positioning system was used to ensure the required sample placement repeatability of 3 μm. Displacement maps were processed using software tools in ImageJ and Python to determine the strain and stress fields. The results allowed the determination of the residual stress-strain state within the sample to the accuracy of about 5%. The notable aspects of the developed technique are its accessibility and effectiveness.

Keywords: Methodology, Indentation, Digital Image Correlation, Plasticity, Residual Stress

INTRODUCTION

One of the main problems in the design of durable and reliable aircraft structures is the need to ensure the fatigue strength of aircraft parts and assemblies [1-4]. Some of the greatest challenges arise at the fixed and separable joints: rivets, bolts, screws, etc. These types of joints are particularly vulnerable to fatigue damage due to two factors: the presence of a stress concentrator (hole) that may promote crack initiation, and the cyclic loads exerted on the airframe during aircraft service [5-7]. As neither the first nor the second factor can be eliminated, methods need to be sought to improve the fatigue resistance of the existing joint designs.

To solve the problem of increasing the fatigue strength of engineering materials under the conditions described above, two groups of effective methods can be distinguished: surface treatment methods and mechanical methods. Both groups focus on increasing crack resistance and slowing down the crack growth by creating fields of compressive residual stress. Surface treatment methods aim to increase fatigue resistance in the near- and sub-surface layers. The advantages of these methods include a wide treatment area with possible improvement of the surface quality, while the disadvantage of this method is the depth of treatment the order of one millimeter. This group includes such methods as: plastic deformation, ultrasonic impact treatment, ion bombardment, polishing, chemical and thermal treatment [8-9]. Mechanical methods also use compressive residual stress fields to increase fatigue strength but focus on the specific point most susceptible to fatigue failure (the technological hole). This

group of methods is distinguished not only by its proven effectiveness, but also by the simplicity of implementing technology into industry. The most well-known mechanical methods are hole drilling, cold expansion methods, vibration processing, high-frequency mechanical peeling, tip crack welding, induction heating with forging, and double dimpling [10-12].

Among the mechanical methods, the cold expansion method (split sleeve) and double dimpling method (StressWave^{TM}) are the most effective and easiest to use. Both methods have proven their effectiveness and can increase the fatigue strength of materials. However, there are several differences that affect technological accessibility and fatigue strength improvement. Although the cold expansion method is the most common way to increase fatigue strength, this technology implies not only the use of a steel rod but also a mandrel with a lubricant [13-14]. This technology requires strict control and is difficult to automate. A major disadvantage of this method is the uneven fields of compressive residual stress along with the thickness of the sample, which reduces the favorable effect [15]. There were some attempts to solve this problem reported using double cold expansion, i.e. cold expansion from both sides [16]. This method was effective in reducing the unevenness of stress distribution over the thickness but significantly complicates the technology. At the same time, the double dimpling technology does not imply any additional equipment besides simple stamping tooling and showing comparable or even superior fatigue strength values compared to double cold expansion [16-17]. Thus, despite its lower popularity at present, double dimpling offers a promising alternative for increasing the fatigue strength of aircraft joints.

There is presently a relatively small number of publications describing the detailed analysis of the dimpling method. Much of the research addresses the quantitative effect of this type of treatment - fatigue life improvement [18-19]. Understanding these mechanisms is critical because the residual stress does not merely alter the mechanical performance through macroscopic load effects - it also influences such structural features as the local strain distribution at the microscale and affects strain hardening in the plastically deformed zones. Such structural changes may contribute synergistically or antagonistically to fatigue resistance improvement. Some articles in the literature describe practical stress-strain analysis using strain gauges [20-22]. However, no articles were found providing detailed analysis of dimpling mechanics and residual stress engineering analysis using Digital Image Correlation, despite the fact shown below that this highly efficient method does not require complex and expensive equipment. Thus, the purpose of this article is to develop a methodology for detailed analysis of deformations and residual stress after double dimpling. With this practical tool in hand, the task of optimizing the double treatment can be tackled.

MATERIALS AND METHODS

The present study focuses on the development of effective and reproducible practical methodology for the determination of the stress-strain state in double dimpled samples. The methods used to conduct the study can be divided into experiment and interpretation. The experimental part consists of machining the samples, applying a speckle pattern, and performing digital image acquisition under identical conditions. The interpretational part consists of processing DIC images, obtaining the displacement dataset, and preforming the calculation of strains and stresses.

Aluminum alloys are most common engineering material in the aerospace industry due to their low density and high corrosion resistance. Aluminum alloys of the Al-Cu-Mg-Mn (or duralumin) system are the most popular among all aluminum alloys in aviation as durable engineering material [23]. That is the reason why samples of aluminum alloy 2024 were studied in this research. Plates 50×50×10 mm in size were coated using standard matte automotive paint for DIC (Fig. 1 a, b). Firstly, white layer was applied as background and afterwards a random speckle pattern was obtained by spraying black paint.

The double-dimpling process was conducted using a 25-ton (250kN) hydraulic rig with tool steel dies (Fig. 1 c, d). Each die incorporated a hardened 16 mm spherical indenter made of 4140 steel.

The reliability of digital image correlation depends primarily on the quality of the acquired images. To ensure consistent imaging conditions, a custom photo box was designed and fabricated (Fig. 1 e). The box was equipped with internal LED lighting to eliminate the influence of external illumination. For stable camera positioning, a Redmi smartphone mount was affixed to the top of the box. Image acquisition was performed using the onboard camera of a Redmi Note 13 Pro smartphone.

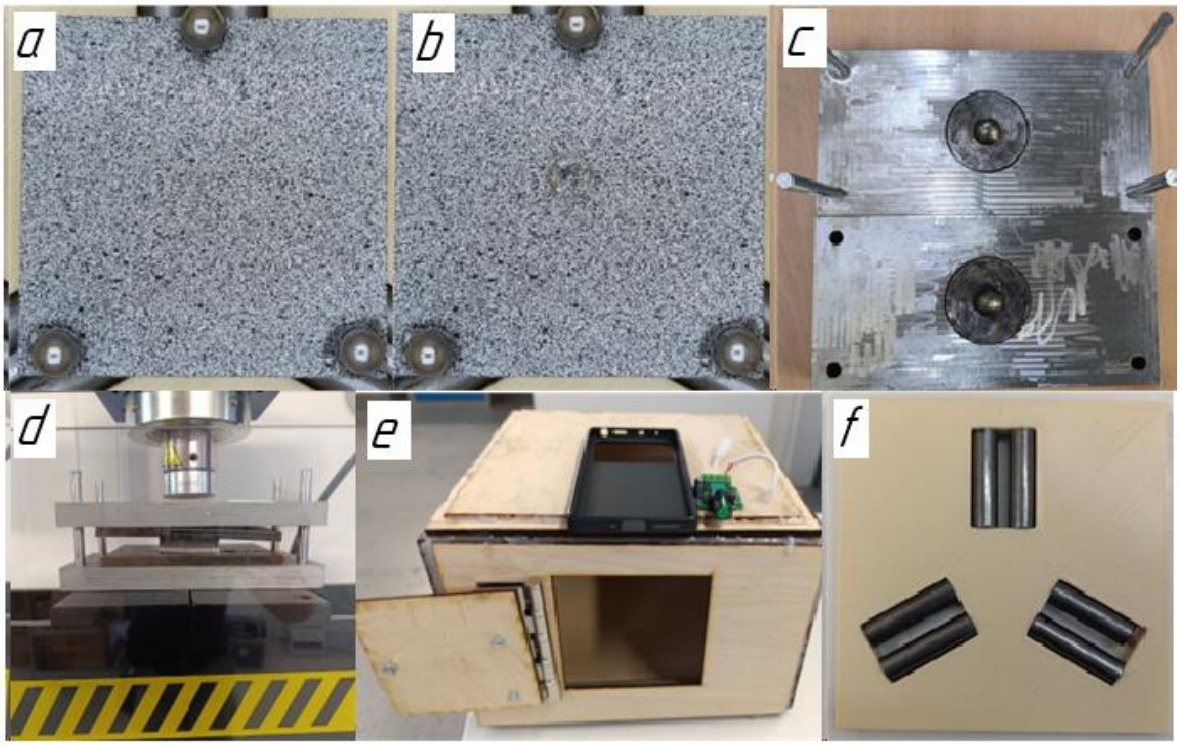

FIGURE 1. Illustration of used materials and equipment
a) Random speckle coating for DIC before dimpling; b) Random speckle coating for DIC after dimpling;
c) Die tooling for double dimpling; d) Die tooling in hydraulic rig; e) Custom photo box;
f) Three-point kinematic positioning system

The main challenge in applying digital image correlation (DIC) to the double-dimpling process is maintaining micron scale sample position reproducibility for taking successive images. Unlike uniaxial tension or bending tests, where continuous imaging can be achieved by positioning a camera in front of the testing machine, the double-dimpling configuration obscures the region of interest with die tooling, preventing *in situ* digital image acquisition. This limitation was addressed through the implementation of a three-point kinematic mounting system. This arrangement ensures full return to the six-sample rigid-body degrees of freedom and provides repeatability in specimen repositioning to ~3μm translational precision (Fig. 1 f).

The analytical processing begins with loading the images in ImageJ program (NIH, Bethesda, MD, USA) and performing DIC to obtain the displacement dataset after dimpling deformation was obtained. Subsequent data processing (removal of rigid body displacement, obtaining 2D displacement maps, error checking and the calculation of strains and stresses) was performed using algorithms written in Python.

RESULTS

The primary objective in developing a new technique for investigating surface effects in dimpling deformation was to determine the method's accuracy. To achieve this, experiments were conducted in two stages: a position-check analysis for quantifying geometric deviations, followed by the dimpling deformation itself for measuring the displacement fields.

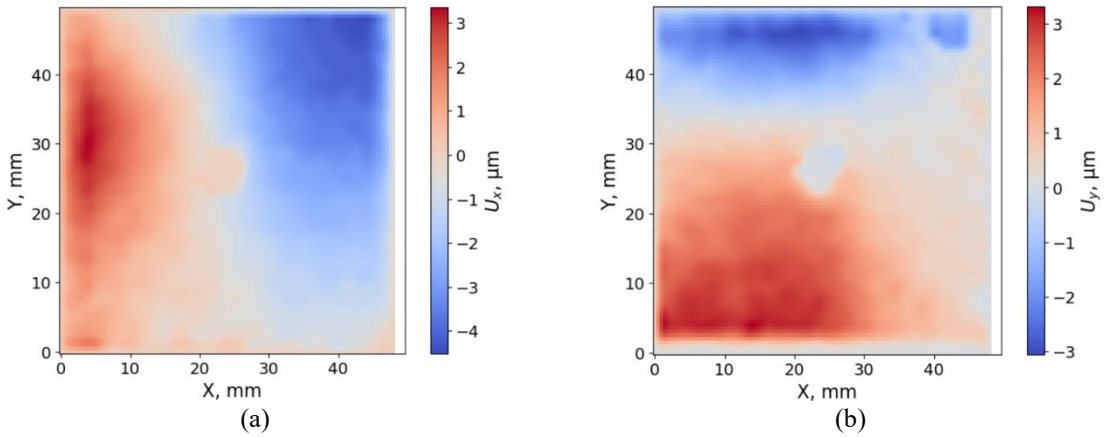

FIGURE 2. Position check analysis Contour maps of displacement errors (a) in the X direction; (b) in the Y direction

Figure 2 presents the results of the first stage, the position-check analysis. In this stage, the initial plate was placed in the photo box and imaged, and the procedure was repeated after a time interval without applying any deformation. The resulting 3D maps (Fig. 2a, b) indicate maximum positional deviations of approximately 3 µm along the X and Y axes.

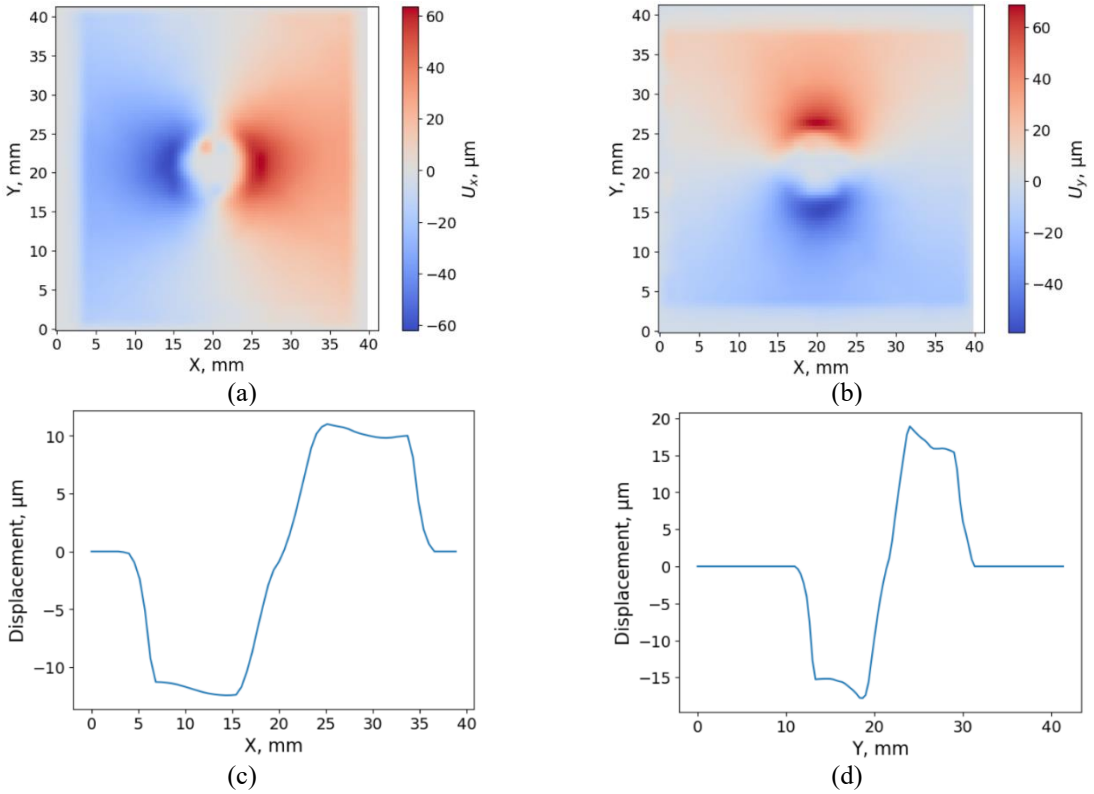

FIGURE 3. Dimpling analysis (a) Reconstructed contour map of displacements in X plane; (b) Reconstructed contour map of displacements in Y plane; (c) Average displacement in X plane; (d) Average displacement in Y plane

Figure 3 shows the displacement results obtained based on digital image comparison before and after sample deformation. The maximum displacement observed after dimpling was about 60 µm (Fig. 3 a, b). Figures 3 c and 3 d show two-dimensional average displacement, exhibiting the expected axisymmetric. The values along the X and Y axes are symmetrically aligned relative to the indentation, and positional deviations have a negligible effect on the measured data. This reproducible distribution confirms the reliability of the experiment and ensures a robust basis for subsequent calculation of deformation and residual stress fields.

The instrumental error of the method was estimated from the maximum aberrations observed during repeated measurements without deformation, which did not exceed 3 μm. In comparison, the main experiment yielded a maximum displacement of approximately 60 μm, indicating a relative error of about 5%. Dividing 3 by 60 equals 0.05. Thus, the camera's instrumental error was estimated to be approximately 5% of the total displacement, which is consistent with standard engineering practice, where a 5% deviation is typical for precision measurement instruments.

Digital Image Correlation (DIC) analysis returns the displacement values at the sample surface in Cartesian coordinates. The next analytical step involved the transformation from Cartesian into cylindrical coordinates system using equations (1-4):

$$r = \sqrt{x^2 + y^2} \tag{1}$$

$$\theta = \arctan2(y, x) \tag{2}$$

$$u_r = u_x \cos\theta + u_y \sin\theta \tag{3}$$

$$u_\theta = -u_x \sin\theta + u_y \cos\theta \tag{4}$$

This problem is considered to be axisymmetric plane stress. The axisymmetric assumption is based on the spherical indenter shape and is validated by the results of DIC displacement after dimpling (Fig. 3 and Fig.4 a). The in-plane stress approximation is justified by two considerations. Firstly, the aluminum plates possess a relatively small thickness (10 mm) compared with their in-plane dimensions (50 × 50 mm²). During the formation of the residual stress field by the double-dimpling method, deformation is highly localized and develops primarily within the specimen plane, as the indenters displace material perpendicular to the surface, producing a predominantly biaxial stress state in the upper layers. Secondly, the deformation occurs under conditions that allow free material flow in the thickness direction, thereby reducing out-of-plane stresses. Together, these factors support the validity of the plane-stress assumption, particularly within the deformation zone.

In this case of axisymmetric plane stress problem, the hoop displacement is thought to be equal to zero and only the radial displacement is of interest.

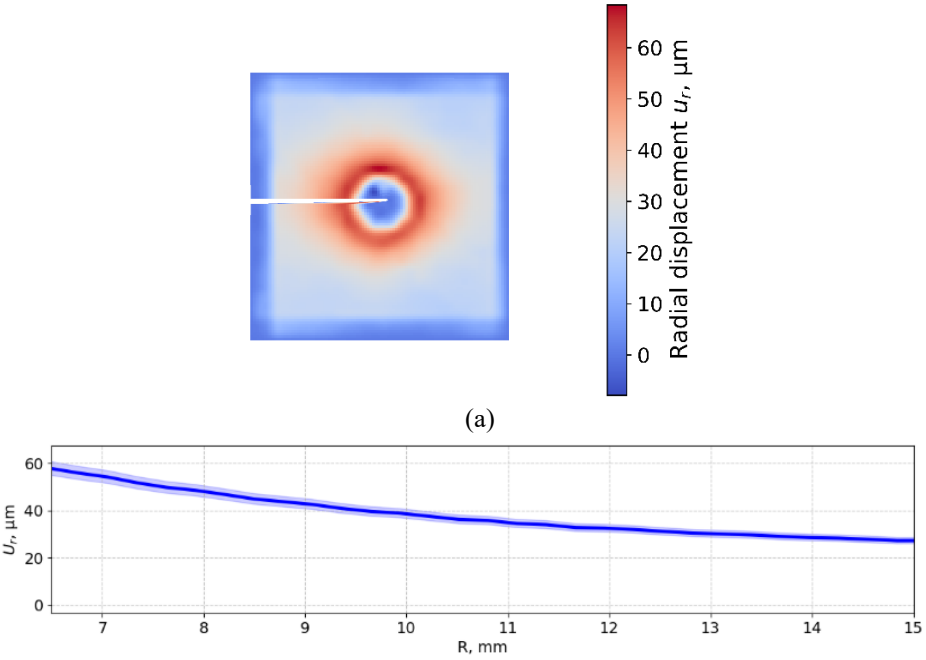

FIGURE 4. Radial displacement a) Reconstructed contour map of radial displacement; b) Line profile of the azimuthally averaged radial displacement

Assuming axisymmetric deformation, the radial and hoop strain components can be calculated using equations (5) and (6):

$$\varepsilon_r = \frac{\partial u_r}{\partial r} \tag{5}$$

$$\varepsilon_\theta = \frac{u_r}{r} \tag{6}$$

One of the restrictions of using DIC was the limitation of the area of investigation. Following dimpling, part of the coated layer may be destroyed or damaged due to the contact between indenter and sample surface under the applied load. To avoid unreliable data, all areas corresponding to the radial position less than 6.5 mm were masked and eliminated from calculations. Also, the 15 mm radial position was identified as the maximum radius of the circle that is fully inscribed within the test sample perimeter. Based on these limitations, all strains were calculated from 6.5 mm to 15 mm radius (Fig. 5).

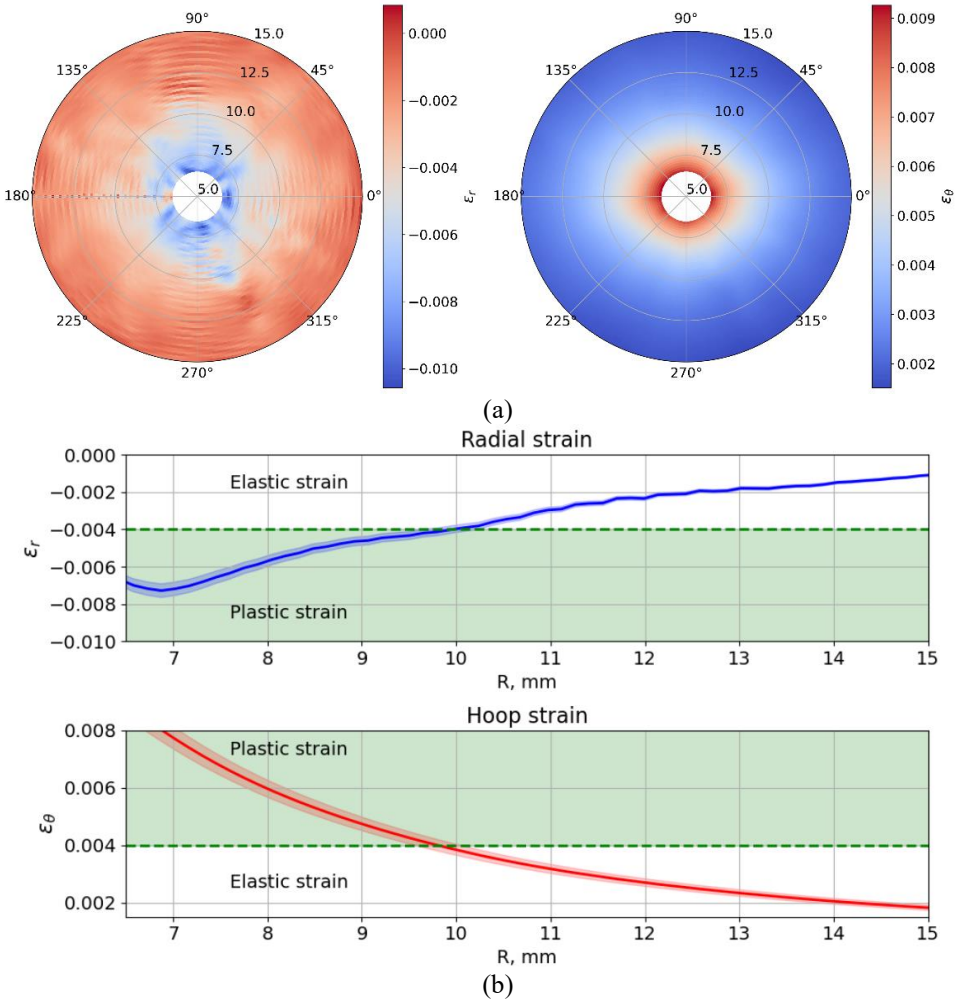

FIGURE 5. Radial and hoop strains (a) Contour maps of strain components (left - radial; right – hoop); (b) Line profiles of the azimuthally averaged strain variation with the approximate identification of the elastic-plastic boundary.

It is well-known that the total strain can be expressed as the sum of elastic and plastic components [24], as given by equation (7):

$$\varepsilon^{total} = \varepsilon^{plastic} + \varepsilon^{elastic} \tag{7}$$

It should be noted at this point that DIC registers the actual physical displacement at the sample surface that may contain contributions from the elastic and plastic effects. Residual stresses are carried only by the elastic part of the strain, as given by Hooke's law. Plastic deformation does not directly carry residual stress after unloading, but it produces the permanent shape changes that lead to the formation of residual stress. Therefore, to evaluate the residual stress after dimpling, the total strain must be decomposed into elastic and plastic components so that only the elastic strain is used to determine the residual stress.

The separation of elastic and plastic strain parts is a major experimental challenge, since the apparent displacements registered by digital imaging are indistinguishable *a priori*. However, to extract maximum useful insight from the experimental observations, the following consideration may be brought to bear upon the task.

The proportionality limit for aluminum alloy 2024-T6 is approximately equal to 280 MPa [25], with Young's modulus of ~ 70 GPa. Consequently, the maximum elastic strain is equal to 0.004 (or 0.4%). Based on this data, 0.004 can be loosely identified as the value that corresponds to the elastic-plastic boundary. Fig.5 (b) illustrates that the strain value of 0.004 is attained around 10 mm radial position, beyond which, at larger radii, the deformation falls into the elastic range. As a simple approximation, further stress calculations are performed for the radial range from 10 to 15 mm. Assuming DIC returns the elastic strain value, it is possible to calculate the radial and hoop stress components for $10 < r < 15$ mm using the plane stress equations (8), (9):

$$\sigma_r = \frac{E}{\left(1-\nu^2\right)}\left[\varepsilon_r + \nu\varepsilon_\theta\right] \tag{8}$$

$$\sigma_\theta = \frac{E}{\left(1-\nu^2\right)}\left[\varepsilon_\theta + \nu\varepsilon_r\right] \tag{9}$$

The data obtained shows that all stress values beyond 10 mm radius are smaller than the elastic limit of aluminum alloy 2024-T6 and reach the maximum magnitude of 200-210 MPa. Residual radial stress is compressive and tends to zero with the increasing radius, while the residual hoop stress is tensile and decreasing towards a non-zero value. This result looks similar to the stress distribution obtained for the solution of the Lamé problem for a thick-walled cylinder under internal pressure [26,27]. Thus, a link may be established between the analytical solution in the Lamé problem and the subject of the present study.

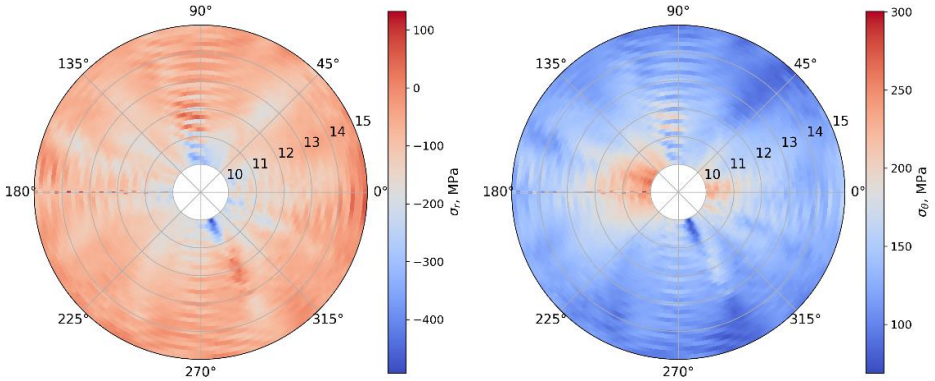

(a)

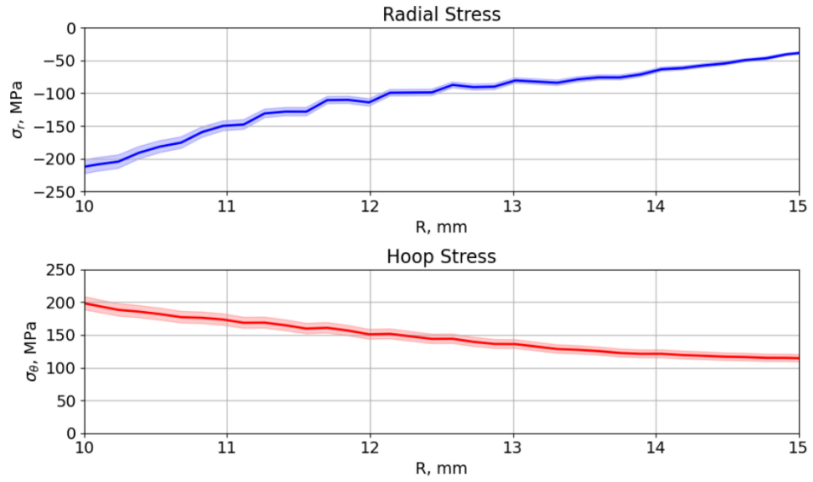

(b)

FIGURE 6. Radial and hoop stress a) Contour maps of stress components (left – radial; right – hoop); b) Line profiles of the azimuthally averaged stress distributions.

Figure 6 shows the reconstructed residual stress component distributions (radial and hoop) as (a) contour maps and (b) average line profiles. Clearly, this represents partial evaluation of the stress state. Complete reconstruction is not possible merely by processing the experimental data, particularly within the domain $r < 10$ mm, where compressive residual stress is expected. Further progress requires either the use of X-ray diffraction methods, or the application of the rational experimental-computational correlation (RECC) [29], i.e. fitting model solution to the observed total strains. This approach will be the subject of a separate study.

DISCUSSION

Using the data obtained from a standard smartphone through DIC analysis makes it possible to evaluate the stress-strain state after 'double dimpling' deformation. To achieve more accurate solutions, it is necessary to perform the rational experimental-computational correlation (RECC) that may involve finite element analysis, X-ray diffraction and electronic speckle-pattern interferometry. The combination of these methods allows verifying the results obtained from DIC and overcoming the limitations of pure experimental data interpretation.

The methodological novelty of this work lies in the application of accessible measurement equipment—a standard smartphone camera—for high-precision analysis of stress-strain fields, thereby eliminating some technological barriers associated with the need for costly specialized instrumentation. The ability to assess quantitatively the efficiency of the processing method opens opportunities for integrating quality control systems directly into manufacturing cycles, ensuring the reliability of processed components.

The scientific significance of the study is determined by the transition from empirical design methods to a scientifically grounded approach based on accurate post-processing measurements and material analysis. This enables more effective implementation of the double dimpling technique to enhance the durability of aerospace structures and to improve quality control in production processes.

The developed methodology establishes a foundation for a deeper understanding of deformation mechanisms and optimization of processing parameters, which is essential for improving the reliability and safety of aerospace engineering applications.

CONCLUSION

In this study, a technique for qualitative and quantitative analysis of deformation and residual stress in aluminum alloys subjected to double dimpling was developed and implemented using digital image correlation (DIC) with a standard smartphone camera. The key advantage of the proposed approach lies in its accessibility, as it eliminates the need for costly specialized equipment; an affordable smartphone and a photo box make the method broadly applicable for research and technological purposes. The technique enables detailed assessment of residual compressive stress distributions, which is critical for enhancing the fatigue strength of aircraft structures. Consequently, the proposed methodology provides new opportunities for the effective analysis and optimization of the double-dimpling process, contributing to improved reliability and operational performance of aerospace components.

ACKNOWLEDGMENTS

This study was carried out under the Agreement for the provision of grant funding from the federal budget for large scientific projects in priority areas of scientific and technological development of the Russian Ministry of Science and Higher Education no. 075-15-2024-552.

REFERENCES

1. S. Maksimovic, K. Maksimovich, I.V. Maksimovic, M. Duric and M. Maksimovich, "Failure analysis of aircraft structural elements", *11th International Scientific Conference on Defensive Technologies Proceedings*, pp. 74–79, Oct. (2024), doi: 10.5937/oteh24015m.
2. S.M.O. Tavares and P.M.S.T. de Castro, "An overview of fatigue in aircraft structures", *Fatigue & Fracture of Engineering Materials & Structures,* vol. **40**, no. 10, pp. 1510–1529, Oct. (2017), doi: 10.1111/ffe.12631.

3. A. Kumar, Prakash C. Patnaik and K. Chen, "Physics of Failures in Aging Aircraft Systems and Components", *Materials of Research Symposium on Physics of Failure for Military Platform Critical Subsystems,* art. **3**, (2021).
4. S.A. Chisholm, A.C. Rufin, B.D. Chapman and Q.J. Benson, "Forty years of structural durability and damage tolerance at Boeing commercial airplanes", *Boeing Technical Journal,* 2017.
5. L. Molent and B. Dixon, "Airframe metal fatigue revisited" *International Journal of Fatigue,* vol. **131**, Art. 105323, (2020), doi.org/10.1016/j.ijfatigue.(2019).105323.
6. A. Venugropal, R. Mohammad, Md F.S. Koslan, A. Shafie, A. bin Ali and O. Eugene, "Crack Growth Prediction on Critical Component for Structure Life Extension of Royal Malaysian Air Force (RMAF) Sukhoi Su-30MKM", *Metals,* vol. **11**, no. 9, (2021), doi: 10.3390/met11091453.
7. A.M. Al-Mukhtar, "Aircraft Fuselage Cracking and Simulation", *Procedia Structural Integrity,* vol. **28**, pp. 124-131, (2020), doi: 10.1016/j.prostr.2020.10.016.
8. S. Lee, Z. Ahmadi, J. W. Pegues, M. Mahjouri-Samani and N. Shamsaei, "Laser Polishing for Improving Fatigue Perfomance of Additive Manufactured Ti-6Al-4V Parts", *Optics & Laser Technology,* vol. **134**, art. 106639, Feb. (2021), doi.org/10.1016/j.optlastec.2020.106639.
9. E.C. Santos, K. Kida, T. Honda, H. Koike and J. Rozwadowska, "Fatigue Strength Improvement of AISI E52100 Bearing Steel by Induction Heating and Repeated Quenching", *Material Science,* vol. 47, pp. 677-382, (2012), doi.org/10.1007/s11003-012-9443-8.
10. K. Zhang, M. Zhu, B. Lan, P. Liu, W. Li and Y. Rong, "The mechanism of high-strength quenching-partitioning-tempering martensitic steel at elevated temperatures", *Crystals,* vol. **9**, no. 2, (2019), doi: 10.3390/cryst9020094.
11. Y. Hu, M. Song, J. Liu and M. Lei, "Effects of stop hole on crack turning, residual fatigue life and crack tip stress field", *Journal of the Brazilian Society of Mechanical Sciences and Engineering*, vol. **42**, no. 5, (2020), doi: 10.1007/s40430-020-02299-1.
12. I. Weich and T. Ummenhofer, "Effects of high-frequency peening methods on the surface layers and the fatigue strength of welded details", *Materials and Manufacturing Processes,* vol. **26**, no. 2, pp. 288-293, (2008), doi.org/10.1080/10426910903386030.
13. R. Su, L. Huang, C. Xu, P. He, X. Wang, B. Yang, D. Wu, Q. Wang, H. Dong and H. Ma, "Factors Influencing Residual Stresses in Cold Expansion and Their Effects on Fatigue Life—A Review", *Coatings*, vol. **13**, art. 2037, (2023), doi: 10.3390/coatings13122037.
14. L. Reid, "Hole cold expansion - The fatigue mitigation game changer of the past 50 years," *Advanced Materials Research*, vols. **891-892**, pp. 679–684, (2014). doi: 10.4028/www.scientific.net/AMR.891-892.679.
15. Q. Li, Q. Xue, Q. Hu, T. Song, Y. Wang, and S. Li, "Cold Expansion Strengthening of 7050 Aluminum Alloy Hole: Structure, Residual Stress, and Fatigue Life", *International Journal of Aerospace Engineering*, vol. **2022**, art. 4057898, (2022), doi: 10.1155/2022/4057898.
16. L. Boni, D. Fanteria, A. Lanciotti, and C. Polese, "Experimental and analytical assessment of fatigue and crack propagation in cold worked open hole specimens", *Fatigue and Fracture of Engineering Materials and Structures*, pp. 930–941, (2013), doi: 10.1111/ffe.12050.
17. E. T. Easterbrook and M. A. Landy, "Evaluation of the StressWave cold working (SWCW) process on high-strength aluminum alloys for aerospace final report" (Air Force research laboratory materials and manufacturing directorate Wright-Patterson Air Force base, 2009). [Online]. Available: http://www.dtic.mil
18. B.D. Flinn, R. Spitsen, D. Kim, T. Nam and E.T. Easterbrook, "Fatigue strength improvement of low carbon steel resistance spot welds by the StressWave™ Process", *SAE Technical Papers,* 2005-01-0903, (2005), doi.org/10.4271/2005-01-0903.
19. E.T. Easterbrook, B.D. Flinn, C.A. Meyer and N. Juhlin, "The StressWave™ fatigue life enhancement process", *SAE Technical Papers,* 2001-01-2578, doi.org/10.4271/2001-01-2578.
20. G. Marannano, A. Pasta, F. Parrinello, and A. Giallanza, "Effect of the indentation process on fatigue life of drilled specimens" *Journal of Mechanical Science and Technology*, vol. **29**, no. 7, pp. 2847–2856, (2015), doi: 10.1007/s12206-015-0613-0.
21. G. Marannano, F. Parrinello, and A. Giallanza, "Effects of the indentation process on fatigue life of drilled specimens: optimization of the distance between adjacent holes" *Journal of Mechanical Science and Technology*, vol. **30**, no. 3, pp. 1119–1127, (2016), doi: 10.1007/s12206-016-0216-4.
22. S.Y. Zhang, J. Schlipf, and A. M. Korsunsky, "Analysis of residual stresses around 'dimpled' cold-expanded holes in aluminium alloy plates", *Materials Science Forum*, pp. 295–300, (2008), doi: 10.4028/www.scientific.net/msf.571-572.295.

23. S. Li, X. Yue, Q. Li, H. Peng, B. Dong, T. Liu, H. Yang, J. Fan, S. Shu, F. Qiu and Q. Jiang, “Development and applications of aluminum alloys for aerospace industry”, *Journal of Materials Research and Technology,* vol. **27**, pp. 944-983, (2023), doi: 10.1016/j.jmrt.2023.09.274.
24. A. M. Korsunsky, *A Teaching Essay on Residual Stresses and Eigenstrains* (Butterworth-Heinemann, Oxford University, 2017), pp. 5-17.
25. T. L. Hursman, “Development of Forming Limit Curves for Aerospace Aluminum alloys” *ASTM STP*, pp.122-149, (1978), doi.org/10.1520/STP30049S.
26. G. Lame, *Leçons sur la Théorie de l’Élasticité* (Gauthier-Villars, Paris, 1852).
27. R.W. Soutas-Little, *Elasticity* (Courier Corporation, Chicago, 2012), pp. 20-50.
28. A. M. Korsunsky, “Residual Elastic Strains in Autofrettaged Tubes: Elastic-Ideally Plastic Model Analysis”, *Journal of Engineering Materials and Technology,* vol. **129**, pp. 77-81, (2007), doi: 10.1115/1.2400267.
29. A.M. Korsunsky, “The Rational Experimental-Computational Correlation (RECC) – reliability improvement toolkit for materials technologies in aerospace design”, in ISSI 2024 Proceedings, Dongguan, China, (2024).